2013 IEEE/RSJ International Conference on
Intelligent Robots and Systems (IROS)
September 14-18, 2014. Chicago, IL, USA,

LINarm: a Low-cost Variable Stiffness Device for Upper-limb Rehabilitation*

Matteo Malosio[1,2], Marco Caimmi[1,2], Giovanni Legnani[2] and Lorenzo Molinari Tosatti[1]

***Abstract*— This paper presents *LINarm*, a device for at-home robotic upper-limb neurorehabilitation. Exploiting peculiar aspects of variable-stiffness actuators, it features functionalities widely addressed by devices specifically designed for assisted rehabilitation as controlled motion, force feedback and safety, together with the low-cost requirement for a widespread installation at patients' home.**

I. INTRODUCTION

A. At-home robot-assisted upper-limb neurorehabilitation

Stroke rehabilitation can take advantage by the exploitation of robotic devices specifically designed to assist the patient and the medical personnel during the recovery. Patients can typically benefit of a period of hospitalization in the first weeks after stroke, during the acute and part of the sub-acute phase, in which neuroplasticity plays an important role in the recovery process. However experimental studies show that plasticity phenomena can be stimulated by robotic intervention even in the chronic phase thus underlying the importance of rehabilitation after discharge [1], [2], [3]. Clinics can afford the purchase of expensive, complex and cumbersome devices, but these same aspects make such devices not suitable to be installed and used at patients' home. The development of widely affordable devices can therefore represent a breakthrough solution to increase the overall quality of recovery for a large amount of stroke patients. Different upper-limb home rehabilitation devices are currently available, but they are typically passive or passively gravity-balanced [4].

Objective of this work is present an active device for upper-limb home rehabilitation. Considering that the upper limb is an incredibly adaptive organ capable of performing numerous functional tasks, one of the first problem to be faced is the selection of the primitive movements to be trained. As most actions involving the use of the upper limb are performed to interact with objects positioned in front of the subject and to eventually take them towards the body, two movements become of particular interest, namely the *reaching* and the *hand-to-mouth*. These two functional movements, which are representative of ADLs like eating and reaching for objects, are correlated with the activity capacity level after stroke [5], [6]. First experiments on a rehabilitation protocol based on these two movements were conducted using an industrial robot [7], [8]. Although the actual complexity of these movements, results refer to that the hand spatial paths may be approximated by straight lines.

B. Force feedback and mechanical compliance

From the invention of the *MIT-Manus* [9], force feedbacks and force-based controls are considered important features for neurorehabilitation devices [10], enabling them to sense and properly react to the actual force exchanged with the patient, in contrast to Continuous Passive Motion devices [11].

By proper control strategies, typically admittance and impedance controls, robots can present tunable and adaptable compliant behaviors on the basis of force-feedback signals, in order to assist patients in performing rehabilitation tasks according to their own impairment levels. Two main approaches are typically adopted to measure externally applied forces/torques: a) measurement by properly installed force/torque sensors or b) estimation through motor currents analysis. While the first one requires the installation of load cells, considerably influencing the overall total cost, the latter one requires the employment of backdrivable transmissions. It is a matter of fact that electric motors are typically efficient at high speed of rotation, requiring mechanical transmissions with not-negligible reduction ratios to increase generated torques and, therefore, affecting the overall transmission backdrivability, unless relatively big and expensive actuators are installed. Without trivializing the aspect, it is partially curious that mechanical compliance is typically obtained by control, instead of by mechanics. Obviously it is not so straightforward as the last sentence seems to suggest: widespread mechanical springs (*e.g.* coil springs) are typically characterized by a nearly constant stiffness, preventing an adjustable level of assistance, feature that is considered important in robotic rehabilitation devices and procedures.

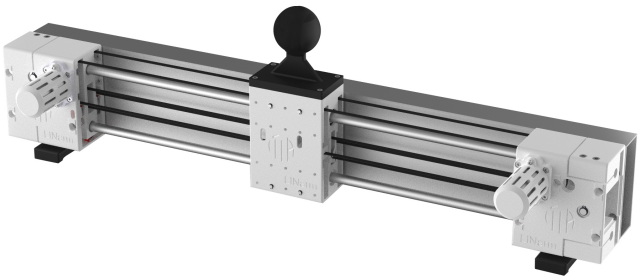

Fig. 1. The *LINarm* device.

*This work was partially supported by the Italian Lombardy region within the *RIPRENDO@home* project.

[1]Matteo Malosio, Marco Caimmi and Lorenzo Molinari Tosatti are with the Institute of Industrial Technologies and Automation of the National Research Council of Italy, via Bassini 15, 20133 Milan, Italy matteo.malosio@itia.cnr.it

[2]Matteo Malosio, Marco Caimmi and Giovanni Legnani are with the University of Brescia, Piazza del Mercato 15, 25121 Brescia, Italy

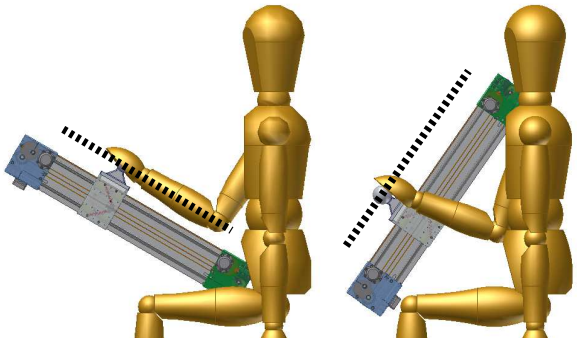

Fig. 2. Examples of *LINarm* installation setups to perform reaching movements (left) and movements towards the body/head (right).

C. Variable Stiffness Actuators

Variable Stiffness Actuators (*VSA*) allow the adjustment, in a controlled manner, of their own mechanical stiffness. A *VSA* is typically made up of two Series Elastic Actuators (*SEA*) arranged in parallel w.r.t. a mobile mass (Fig.3). A *SEA* is, in general terms, made up of a rigid actuator and an elastic element (*e.g.* a spring) arranged serially. Two *SEA* featuring non-linear stiffness, arranged in parallel and exerting opposite forces, characterize a typical *VSA*. *SEA* stiffness nonlinearity is required to make the *VSA* stiffness adjustable [12]. The use of *VSA*, already adopted in different applications not requiring high positioning precision, can lead to the following features, considered really important for rehabilitation devices:

- *adjustable stiffness* requiring neither force sensors nor transmission backdrivability;
- *force estimation* by position sensors (*e.g.* potentiometers), typically cheaper than force sensors, being known the spring characteristic;
- suitability for a *direct interaction with human beings* since intrinsic mechanical compliance avoids high impulsive forces in case of malfunctioning or undesired movements.

D. LINarm

On the basis of these premises the authors came up to the idea of designing the *LINarm* (Fig. 1), a low-cost device to perform *LIN*ear rehabilitation exercises of the human *arm*, hence the name, exploiting peculiar features of *VSA*, and allowing linear rehabilitation movements along different directions, as *reaching* and *hand-to-mouth*, according to its installation setup (Fig. 2). In order to describe its main characteristics, this paper deals with the mechanical functioning (Sec.II), the control features (Sec.III) and the key aspects of the prototype design (Sec.IV).

II. MECHANICS

In this section the mechanical scheme of *LINarm* is described: a *VSA* controlled by two *SEA* with a non-linear stiffness characteristic, determines the motion and the stiffness of the end-effector of the device (Fig.3). Both the end-effector position and stiffness can be adjusted properly

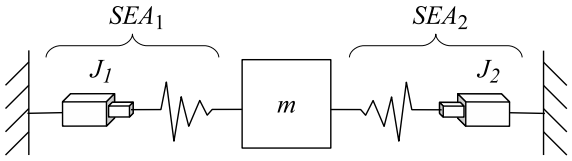

Fig. 3. Typical scheme of a *VSA*: two non-linear *SEA* arranged in parallel can control the position and the stiffness of a mobile mass m.

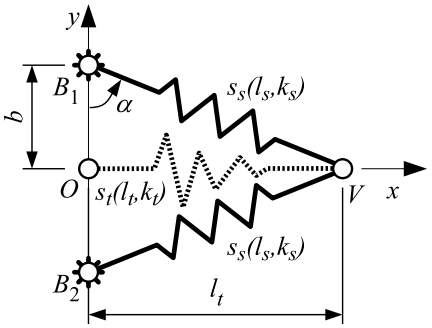

Fig. 4. Kinematic scheme of the non-linear *triangular spring* employed to realize non-linear *SEA* in *LINarm*.

controlling in position the *SEA*, increasing the overall stiffness as the tension force applied by *SEA* to the end effector increases. The *SEA* employed in *LINarm* are denoted as *triangular springs* (Sec.II-A), for their characteristic shape, whose coupled configuration is, for the same reason, denoted as *quadrangular spring* (Sec.II-B), realizing the *VSA*.

A. Triangular spring

Referring to Fig. 4, two linear[1] coil springs s_s, arranged in parallel and symmetrically to the x-axis, hinged to two points B_i $(i = 1, 2)$ lying on the y-axis, both connected to a point V translating along the x-axis, realize the virtual easily-affordable zero-length[2] non-linear spring s_t, connecting point O to point V. It was chosen to use two linear springs instead of a single nonlinear one thanks to their wide availability on the market. Moreover, this configuration allows to have $O \equiv V$. Let us denote by:

- $l_{s,0}$ the free length of spring s_s;
- k_s the stiffness of spring s_s;
- l_t the length of the virtual spring s_t;
- k_t the stiffness of the virtual spring s_t;
- $b = \overline{OB_i}$ the half distance between endpoints hinged to the ground;
- $l_s = \overline{B_iV} = \sqrt{l_t^2 + b^2}$ the length of coil spring s_s;
- $\alpha = \arctan(l_t/b)$ the angle between the axis of spring s_s and the y-axis.

The tension force exerted by each spring s_s is

$$f_s = k_s(l_s - l_{s,0}) \tag{1}$$

[1]In this discussion the stiffness of coil springs is approximated as constant. To reduce possible approximation errors affecting the functioning of the device in real use, the VSA stiffness will be calibrated through the use of a dynamometer, experimentally obtaining the mechanical characteristics depicted in Fig. 7 and Fig. 8.

[2]The term *zero-length spring* denotes a spring exerting zero force if it has zero length.

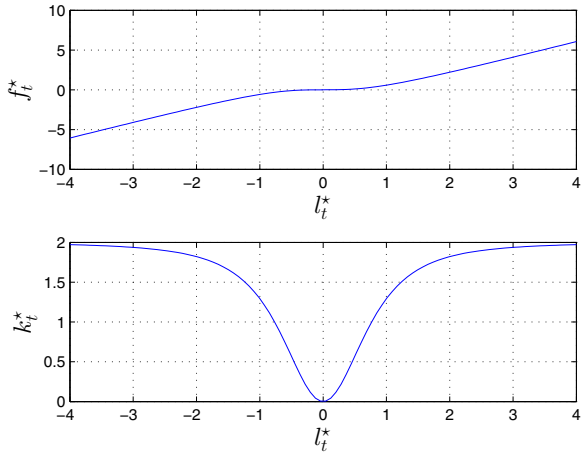

Fig. 5. Normalized tension force $f_t^\star$ and stiffness $k_t^\star$ of s_t as function of the normalized elongation $l_t^\star = l_t/b$, assuming $k_s = 1$ and $l_{s,0} = b$.

and, consequently, the force exerted by s_t is

$$f_t = 2 f_s \sin\alpha = \frac{2\, l_t\, k_s \left(\sqrt{{l_t}^2 + b^2} - l_{s,0}\right)}{b\sqrt{\frac{{l_t}^2}{b^2} + 1}}. \qquad (2)$$

Due to its non-linear characteristic, two distinct stiffness values can be evaluated:

- a differential stiffness k_t, locally referred to any point of the spring stroke

$$k_t = \frac{d}{dl_t} f_t; \qquad (3)$$

- an avarage stiffness $\overline{k_t}$, considering the required force f_t to achieve a certain total elongation l_t

$$\overline{k_t} = \frac{f_t}{l_t}. \qquad (4)$$

Normalized tension force and stiffness of s_t are represented in Fig. 5.

B. Quadrangular spring

In *LINarm* two equal *triangular springs* are arranged in parallel w.r.t. the end effector of the device, featuring a *VSA*, denoted by *quadrangular spring* s_q. Referring to Fig. 6 let us denote by s_{ti}, f_{ti} and k_{ti} $(i = 1, 2)$ the two non-linear *triangular springs*, their tension force and stiffness, respectively. The resulting applied force f_q to the m body (*i.e.* the device handle) and the resulting stiffness k_q of s_q are

$$f_q = f_{t1} + f_{t2} \qquad k_q = k_{t1} + k_{t2}. \qquad (5)$$

Let us denote by x_m the actual position of the mobile platform m along the x-axis and by x_e its equilibrium position if no external force is applied to it. Neglecting inertial effects and taking into account the symmetry of the system, $x_e = (x_1 + x_2)/2$. Let us moreover denote the displacement of m from the equilibrium position (occurring

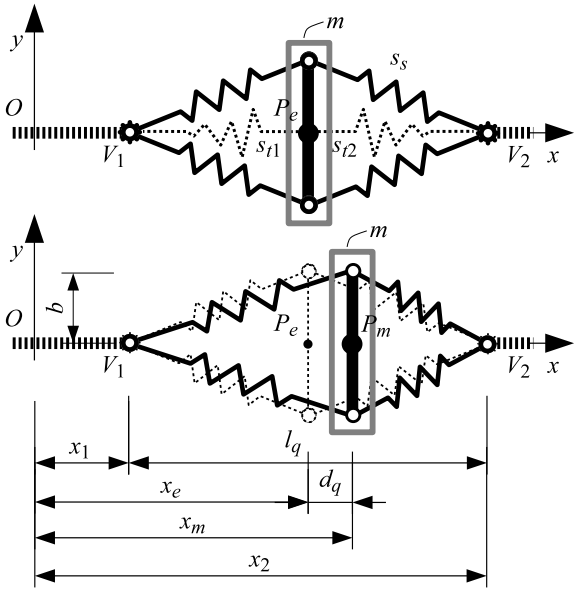

Fig. 6. Two *triangular springs* s_{t1} and s_{t2} arranged in parallel realize the *quadrangular spring* s_q employed in *LINarm* to obtain the *VSA*. The position and the mutual distance between the endpoints V_1 and V_2 define the position of the equilibrium point P_e and the stiffness k_q of the end effector m.

if an external force is applied) by $d_q = x_m - x_e$ and the distance between endpoints V_1 and V_2 of s_q by $l_q = x_2 - x_1$.

The stiffness k_q can be evaluated partially differentiating f_q w.r.t. d_q and l_q:

$$k_{q,d} = \frac{\partial}{\partial d_q} f_q \qquad k_{q,l} = \frac{\partial}{\partial l_q} f_q, \qquad (6)$$

The normalized tension force $f_q^\star$ and stiffness $k_q^\star$ are depicted in Fig. 7 and Fig. 8, respectively.

III. CONTROL

A simplified representation of the *LINarm* mechatronic system is represented in Fig. 9. The control system is in charge of controlling in real time both the equilibrium position x_e and the stiffness k_q of the device, controlling the actuators positions q_1 and q_2. As previously described, x_e is the mid point between V_1 and V_2, and the relation between k_q, x_1 and x_2 can be inferred from Fig. 8.

In addition, measuring the displacement d_q of m from its equilibrium point P_e and the distance l_q, between V_1 and V_2, it is possible to estimate the force f_m externally applied to m (Fig. 7), exploiting it as a force-feedback signal (Fig. 10). Referring to Fig. 11, the control of the stiffness k_q (Fig. 11(a)), exploiting the variable-stiffness actuator characteristic, can be enhanced including an admittance control scheme exploiting the force-feedback signal f_m (Fig. 11(b)), emulating a spring s_c configured in series to s_q (Fig. 11(c)). Given a desired stiffness k_d, it is therefore possible to properly tune k_q and k_c through the relation

$$k_d = (k_c^{-1} + k_q^{-1})^{-1}, \qquad (7)$$

enhancing the stiffness control available considering only s_q.

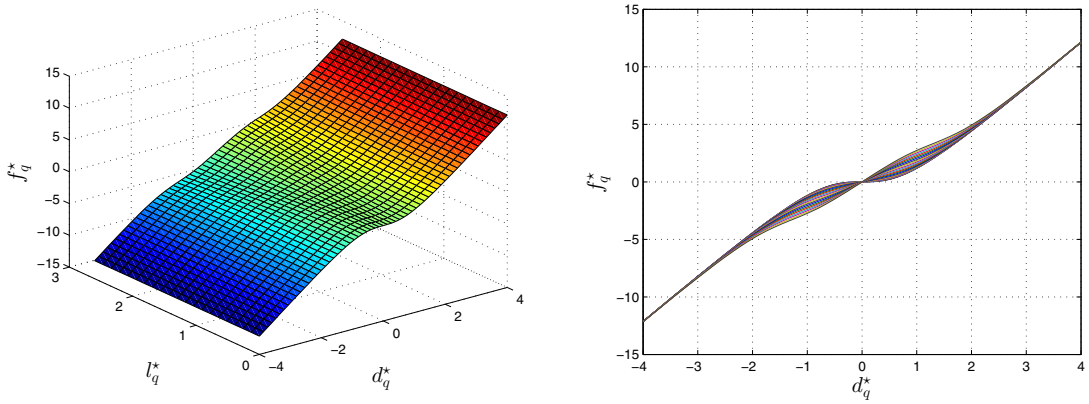

Fig. 7. Normalized tension force $f_q^\star$ of s_q as function of $d_q^\star = d_q/b$ and $l_q^\star = l_q/b$, assuming $k_s = 1$ and $l_{s,0} = b$.

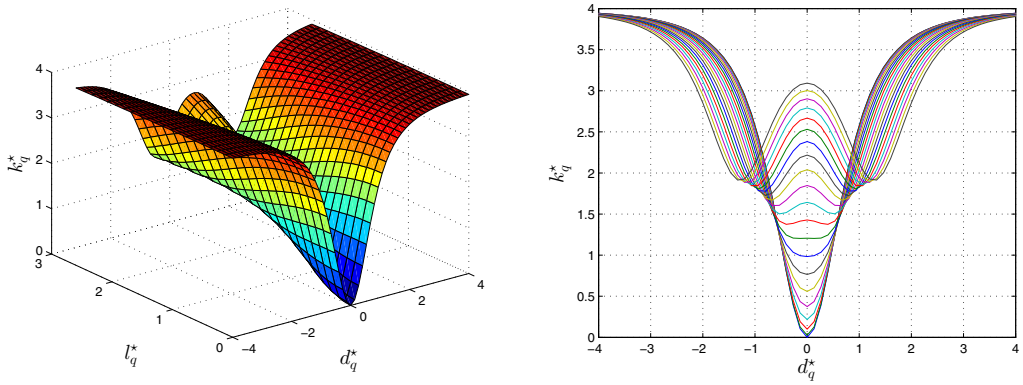

Fig. 8. Normalized stiffness $k_q^\star$ of s_q as function of $d_q^\star = d_q/b$ and $l_q^\star = l_q/b$, assuming $k_s = 1$ and $l_{s,0} = b$. It varies from 0, if all coil springs s_s are parallel to the y-axis ($d_q = 0$ and $l_q = 0$), to 4, if all s_s are parallel to the x-axis ($d_q \to \infty$ or $l_q \to \infty$).

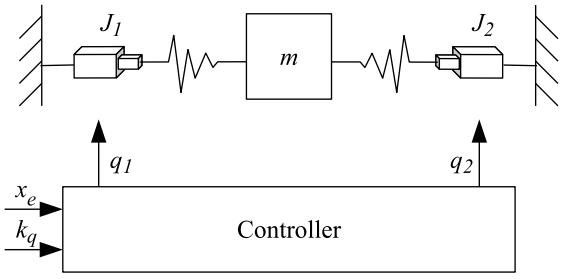

Fig. 9. The position x_e of the end-effector equilibrium point and its stiffness k_q are defined controlling in position the two actuators.

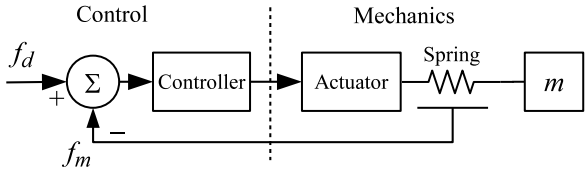

Fig. 10. An impedance control loop is feasible exploiting the value of the externally applied force, estimated on the basis of the displacement d_q of m from its equlibrium point.

IV. LINARM PROTOTYPE DESIGN

LINarm has been designed taking into account both functional and low-cost requirements, in order to actually realize an affordable device, both from the mechanical and the electrical point of view, minimizing material, production and assembly costs.

The prototype (Fig. 1) is actuated by two cheap rotational motors (*Pololu 131.25:1 Metal Gearmotor 37Dx57L mm, 80 RPM, 1.8Nm, 12V*) equipped by an internal incremental rotary encoder (64 counts per revolution of the high speed shaft, corresponding to 8400 c.p.r. of the low speed shaft), assembled at the extremities of the *LINarm*, as represented in Fig. 12. The motors transmit linear motions to s_q endpoints V_1 and V_2 by two synchronous belt systems, whose position measurement resolution is $E_{l,q} = 0,02mm$, determined by the encoder resolution and the diameter of the driving pulley ($180mm$). A detailed view representing the *LINarm* end effector is depicted in Fig. 13. The handle is linearly constrained by four linear bushings sliding on two parallel shafts. The *quadrangular spring* s_q is made up of four

(a) The stiffness k_q of the *LINarm* end effector can be controlled directly by the *VSA*.

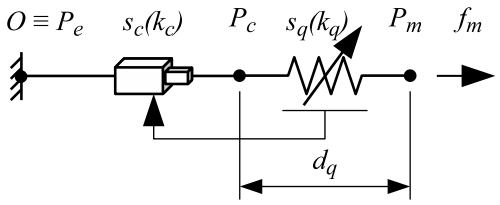

(b) The externally applied force f_m can be estimated measuring the displacement d_q of the end effector from its equilibrium position and used as a force-feedback signal.

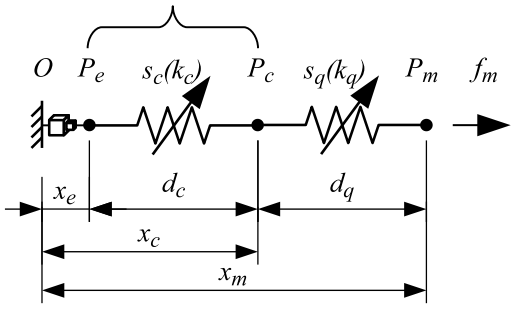

(c) The value of f_m allows to control the actuators according to an admittance control scheme, realizing an additional virtual spring s_c configured in series to s_q.

Fig. 11. The stiffness control of the *LINarm* end effector can be enhanced through an admittance control scheme.

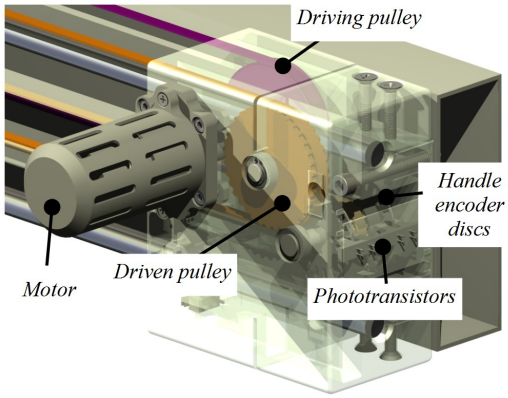

Fig. 12. Assembly of one of the motorized extremities of the device.

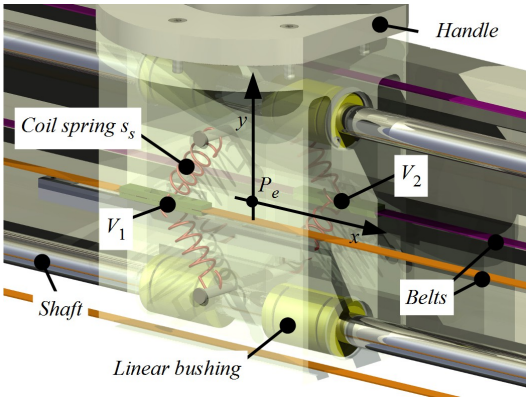

Fig. 13. Detailed view of the *LINarm* end effector and *VSA*. Two synchronous belt systems transmit the motion to the non-linear *SEA*. The other five degrees of freedom of the end effector are constrained by four linear bushings sliding along two parallel shafts.

coil springs s_s (*Vanel, U.091.085.0444.A*) characterized by $k_s = 0.25N/mm$, $l_{s,0} = b = 44.4mm$ and $l_{s,max} = 150.4mm$, denoting by $l_{s,max}$ their maximum length. The considered values allows to theoretically adjust the mechanical stiffness of s_q in its equilibrium position ($d_q = 0mm$) between $k_{q,min} = 0N/mm$, if $l_q = 0mm$, and $k_{q,max} = 0.98N/mm$, if $l_q = 287mm$ (s_s completely extended). As previously mentioned, an experimental calibration of the global stiffness will be performed to take into account mechanical nonlinearities. Proper mechanical end-strokes will limit the maximum spring elongation to avoid breakage and, consequently, risky accelerations. The total length of the prototype is $800mm$, leading to a maximum stroke of $600mm$. The linear position of the handle is measured by a low-cost incremental encoder made up of two discs realized in plastic, perforated in quadrature, and whose angular positions are measured by two phototransistors. The measurement resolution is $E_{d,q} = 0,95mm$, determined by the encoder resolution (84 c.p.r.) and the circumference of the handle driven pulley ($80mm$). The relapse of measurement uncertainties $E_{l,q}$ and $E_{d,q}$ on force estimation and stiffness control is shown in Fig. 15.

The end effector is equipped by an interchangeable ergonomic handle to guarantee a firm and comfortable grasp by the patient. Some mechanical components are specifically designed to be fabricated in plastic and 3D-printed. Printing techniques will in fact facilitate the production and distribution of small-medium production lots of the *LINarm* during its multicenter evaluation and initial commercialization phase, making also possible the auto-production of the device.

The electrical layout and connections are represented in Fig. 14. The control system is implemented in an *Arduino-Due* microcontroller board, in charge of closing control loops in real time and controlling motors *M1* and *M2* through the *Pololu Dual VNH5019 Motor Driver Shield*. Two phototransistors *PS1* and *PS2* measures the handle encoder position and six microswitches *MSi* are used as end-strokes and to reset encoders positions. The control system is implemented exploiting the open-source *ChibioOS/RT* Real-Time Operating System, compiled for the *ARM Cortex-M3 CPU*. A low-cost and compact ARM-based computer (*A20-OLinuXino-MICRO*), interfaced to the Arduino board through a serial connection, is in charge of high-level functionalities control, exercises programming and rendering of an engaging virtual environment. Exploiting the possibility of implementing a direct synchronous communication between two Arduinos

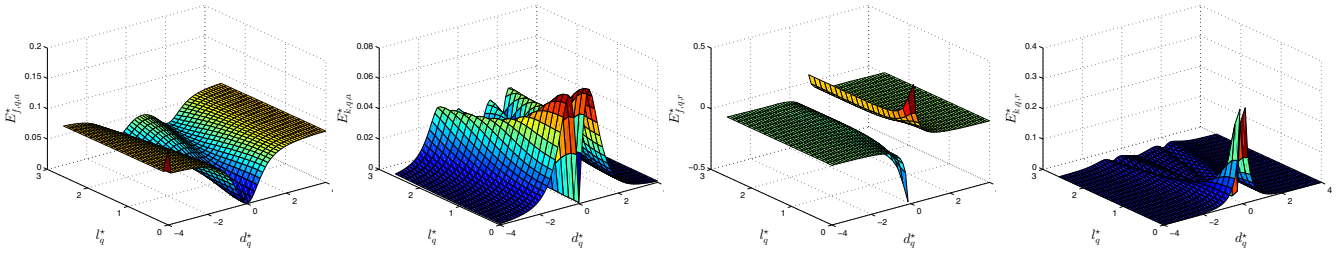

Fig. 15. Normalized maximum force $E^{\star}_{f,q}$ and stiffness $E^{\star}_{k,q}$ estimation errors determined by position measurement uncertainties of the *LINarm* prototype. Both absolute (subscript a, leftmost graphs) and relative (subscript r, rightmost graphs) errors are reported. Relative errors are relevant if force and stiffness values are low ($d^{\star}_q \approx 0$ and $l^{\star}_q \approx 0$). Absolute errors remain confined. Encoder resolutions influences the precision of estimating low forces. The greater influence on error estimation is caused by the handle encoder because its precision is not increased by any mechanical reducer, as it is in the motor encoder.

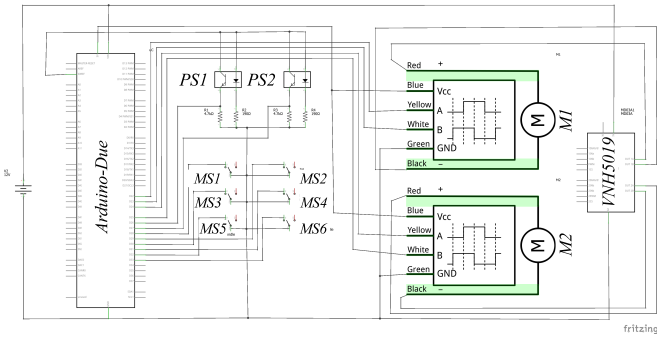

Fig. 14. Electrical components and connections.

through the I^2C serial protocol, the coordinate motion of two distinct devices will be moreover implemented, to perform assisted bilateral exercises using both upper limbs.

V. CONCLUSIONS

LINarm is a device for upper-limb rehabilitation featuring force-feedback and variable-stiffness assistance. Specific benefits derive from its variable-stiffness architecture: adjustable compliance, safety, suitability to human-robot interaction, cheapness, lightness and compactness. The first prototype is currently been assembled. Successively, it will be experimentally evaluated by healthy subjects and, furtherly, clinically assessed in real clinical trials with stroke patients with different functional levels. Exploiting its cost-effectiveness, it will be afterward reproduced and distributed to a selected set of patients to carry out experimental trials in the domestic environment.

ACKNOWLEDGMENTS

The authors would like to thank João Carlos Dalberto, Francesco Paolucci and Giulio Spagnuolo for the support to the mechanical design and the realization of the *LINarm* prototype, and Roberto Bozzi for its electrical wiring.

REFERENCES

[1] N. Hogan and H. I. Krebs, "Interactive robots for neuro-rehabilitation," *Restor. Neurol. Neurosci.*, vol. 22, no. 3-5, pp. 349–358, 2004.

[2] S. Mazzoleni, P. Sale, M. Tiboni, M. Franceschini, M. C. Carrozza, and F. Posteraro, "Upper limb robot-assisted therapy in chronic and subacute stroke patients: a kinematic analysis," *Am J Phys Med Rehabil*, vol. 92, pp. 26–37, Oct 2013.

[3] R. Colombo, I. Sterpi, A. Mazzone, C. Delconte, and F. Pisano, "Robot-aided neurorehabilitation in sub-acute and chronic stroke: does spontaneous recovery have a limited impact on outcome?," *NeuroRehabilitation*, vol. 33, pp. 621–629, Jan 2013.

[4] A. Prochazka, "Passive devices for upper limb training," in *Neurorehabilitation Technology*, pp. 159–171, Springer, 2012.

[5] M. Alt Murphy, C. Willen, and K. S. Sunnerhagen, "Movement kinematics during a drinking task are associated with the activity capacity level after stroke," *Neurorehabil Neural Repair*, vol. 26, no. 9, pp. 1106–1115, 2012.

[6] M. Caimmi, S. Carda, C. Giovanzana, E. S. Maini, A. M. Sabatini, N. Smania, and F. Molteni, "Using kinematic analysis to evaluate constraint-induced movement therapy in chronic stroke patients," *Neurorehabil Neural Repair*, vol. 22, no. 1, pp. 31–39, 2008.

[7] A. Scano, M. Caimmi, M. Malosio, N. Pedrocchi, F. Vicentini, L. Molinari Tosatti, and F. Molteni, "Upper limb robotic rehabilitation: Treatment customization," *Gait & posture*, vol. 37, no. S1, pp. S13–S14, 2013.

[8] M. Caimmi, N. Pedrocchi, A. Scano, M. Malosio, F. Vicentini, L. Tosatti, and F. Molteni, "Proprioceptivity and upper-extremity dynamics in robot-assisted reaching movement," in *Biomedical Robotics and Biomechatronics (BioRob), 2012 4th IEEE RAS EMBS International Conference on*, pp. 1316–1322, 2012.

[9] H. Krebs, N. Hogan, B. Volpe, M. Aisen, L. Edelstein, and C. Diels, "Overview of clinical trials with mit-manus: a robot-aided neuro-rehabilitation facility," *Technology and Health Care*, vol. 7, no. 6, pp. 419–423, 1999.

[10] L. Marchal-Crespo and D. J. Reinkensmeyer, "Review of control strategies for robotic movement training after neurologic injury.," *Journal of neuroengineering and rehabilitation*, vol. 6, pp. 20+, June 2009.

[11] B. T. Volpe, M. Ferraro, D. Lynch, P. Christos, J. Krol, C. Trudell, H. I. Krebs, and N. Hogan, "Robotics and other devices in the treatment of patients recovering from stroke," *Curr Atheroscler Rep*, vol. 6, pp. 314–319, Jul 2004.

[12] B. Vanderborght, A. Albu-Schaeffer, A. Bicchi, E. Burdet, D. G. Caldwell, R. Carloni, M. Catalano, O. Eiberger, W. Friedl, G. Ganesh, M. Garabini, M. Grebenstein, G. Grioli, S. Haddadin, H. Hoppner, A. Jafari, M. Laffranchi, D. Lefeber, F. Petit, S. Stramigioli, N. Tsagarakis, M. Van Damme, R. Van Ham, L. C. Visser, and S. Wolf, "Variable impedance actuators: A review," *Robot. Auton. Syst.*, vol. 61, pp. 1601–1614, Dec. 2013.